# Evaluation of MRI artifacts caused by metallic dental implants and classification of the dental materials in use

[1] Z. Starčuk, [1]K. Bartušek, [2]H. Hubálková,
[4]T. Bachorec, [1]J. Starčuková, [3]P. Krupa

[1] Institute of Scientific Instruments, Academy of Sciences of the Czech Republic,
Královopolská 147, 61264 Brno, Czech Republic
E-mail: *starcuk@isibrno.cz*
[2] Clinic of Stomatology, 1st Faculty of Medicine, Charles University in Prague,
Kateřinská 32, 12108 Praha 2, Czech Republic
E-mail: *hana.hubalkova@lf1.cuni.cz*
[3] St. Anne University Hospital, Pekařská Brno, Czech Republic
E-mail: *pkrupa@med.muni.cz*
[4] SVS FEM s.r.o., Čechyňská 25, 60200 Brno, Czech Republic

**Abstract.** *Metallic objects (dental fillings, crowns, fixed bridges etc.), now found in many patients, may become a reason for the patient's ineligibility for MR examination because of safety or image artifact concerns. The severity of the MRI artifacts caused by these objects depends primarily on the material, shape, position and orientation of the object, MRI method applied, and the location of the tissues of interest. The purpose of this work is to demonstrate the artifacts and describe a method of measuring the relevant material properties and the results. A method for the measurement of magnetic susceptibility based on field distortion simulation and field mapping based on MRI is described. Objects made of several materials were tested experimentally and these results were checked against simulated results. It has been found that among the more than 100 dental materials currently in use there are highly paramagnetic materials (Ni-Cr or Co-Cr based alloys), in which $B_0$ inhomogeneity effects dominate, as well as slightly diamagnetic materials (alloys of precious metals and amalgams), which may cause artifacts due to the RF field inhomogeneity arising from induced RF currents. Spatial mapping of these effects may give indication of potential hot spots in these objects.*

*Keywords: magnetic resonance imaging, artifacts, metallic implants, dental alloys, magnetic susceptibility*

## 1. Introduction

*Purpose*
Metallic objects (dental crowns, fixed bridges, splints, surgical fixtures, micromeshes, microplates and clips) are often encountered in the orofacial region of patients indicated for MR examination. Dental implants are used in reconstruction of prosthetic defects in the oral cavity and in modern surgical methods in traumatology. These appliances present a concern from the point of view of patient's safety and MR data quality. Depending on their shape, orientation, material, and the type of measurement, these objects may be negligible as well as deleterious. The knowledge of the behaviour of these objects in the MR environment is needed for the assessment of the risks involved and of a patient's eligibility for MR examination. The importance increases in high-field clinical systems. The goal of this work was to test the behavior of dental crowns and other samples made of various materials in vitro, to model the effects and use the model and experiment data to determine the relevant material properties.

*Theory*

Artifacts. Image artifacts caused by the metallic objects are due to the induced inhomogeneity of either the static ($B_0$) or the RF field ($B_1$). In standard measurements, the $B_0$ inhomogeneity effects are twofold: slice distortion in measurements with slice selection (2D MRI, slice defined by condition $\omega_{ctr}-\Delta\omega/2 < \gamma.g_s.r_s+\gamma.B_{dz}(\mathbf{r}) < \omega_{ctr}+\Delta\omega/2$, where $\omega_{ctr}$ is the slice-selection RF pulse offset, $\Delta\omega$ its bandwidth, $g_s$ is the slice-selection field gradient, and $B_{dz}$ is the z-component of the static field distortion) and image distortion (spins in real position $\mathbf{r}$ are displaced along the readout direction into image position $\mathbf{r'} = \mathbf{r}+\mathbf{u}_r.B_{dz}(\mathbf{r})/g_r$). Detailed mathematical treatment is available [1]. The RF currents induced in conducting objects produce local magnetic fields of the same frequency and may cause local inhomogeneity of excitation.

Static field. The magnetic field at a position $\mathbf{r}$ generated by a distribution of dipoles in a medium is the sum of the fields generated by each dipole. It can be practically calculated in a the Fourier domain ($\mathbf{k}$-space), as demonstrated by Deville *et al.* [2] and Marques *et al.* [3], as

$$B_{dz}(\mathbf{r}) = B_0\ FT_\mathbf{k}^{-1}\{FT_\mathbf{r}\{\chi(\mathbf{r})\}(\mathbf{k}) . K(\mathbf{k})\}(\mathbf{r}), \qquad (1)$$

where $\chi(\mathbf{r})$ is the spatially varying magnetic susceptibility, $K(\mathbf{k}) = \cos^2(\beta)-\frac{1}{3}$ and $\beta$ is the angle between the direction of the main magnetic field and $\mathbf{k}$. This formula gets simplified for a sample containing two homogeneous media. If a tested object of magnetic susceptibility $\chi_s$, whose shape is characterized by a mask $V(\mathbf{r})$ equal to 1 in its interior, is immersed in a much larger volume of water of magnetic susceptibility $\chi_w= -9.05\times10^{-6}$, the field change is described as

$$B_{dz} = (\chi_s - \chi_w)\ B_0\ FT^{-1}\{FT\{V\} . K\} \qquad (2)$$

Experimentally, the field distortion around an inserted object can be determined from gradient-echo images, in which the image phase accumulates the frequency offset evolution during the echo-time *TE*. If the slice-selection gradients $g_s$ is high enough to render the slice-localization error negligible, the same slice of a water-filled phantom can be measured with an identical GE pulse sequence without and with the test object inserted. In image areas with sufficient signal intensity, the image phases are $\Phi(\mathbf{r})$ and $\Phi'(\mathbf{r'}) = \Phi(\mathbf{r}) + \gamma B_{dz}(\mathbf{r}).TE$, respectively, which can be used for finding the unknown $B_{dz}(\mathbf{r})$ for each position $\mathbf{r}$. After substituting for $\mathbf{r'}$ and unwrapping the phases, the equation can be solved iteratively. A simpler approach is possible if the displacement is well below the pixel size. In such a case $\mathbf{r'}\approx\mathbf{r}$ and $\Delta\Phi(\mathbf{r}) := \Phi'(\mathbf{r})-\Phi(\mathbf{r}) \approx \gamma B_{dz}(\mathbf{r}).TE$, from which the field distortion is

$$B_{dz} = \Delta\Phi / (\gamma\ TE). \qquad (3)$$

By matching the field map data $B_{dz}$ from Eq. 3 and the theoretical values of Eq. 2, the magnetic susceptibility of the object tested can be determined.

## 2. Subject and Methods

Dental crowns and cylindrical samples (20 mm length, 4 mm diameter) made of several materials were attached to plastic holders and immersed in water. Gradient echo (GE) and spin echo (SE) images were measured in various orientations in 4.7 T and 1.5 T systems and the results were compared with numerical models [1,2]. Among the commercial materials tested there were (1) alloys of precious metals (Au, Pt, Ag, Ir, Pd), (2) alloys of non-precious metals (Co-Cr, Ni-Cr), and (3) amalgams (Hg+Ag-Sn-Cu). ANSYS (ANSYS Inc., Canonsburg, PA) was used for RF modeling. The RF effects were tested in experiments with rotated linearly polarized $B_1$ coil and in measurements with incremented flip angles.
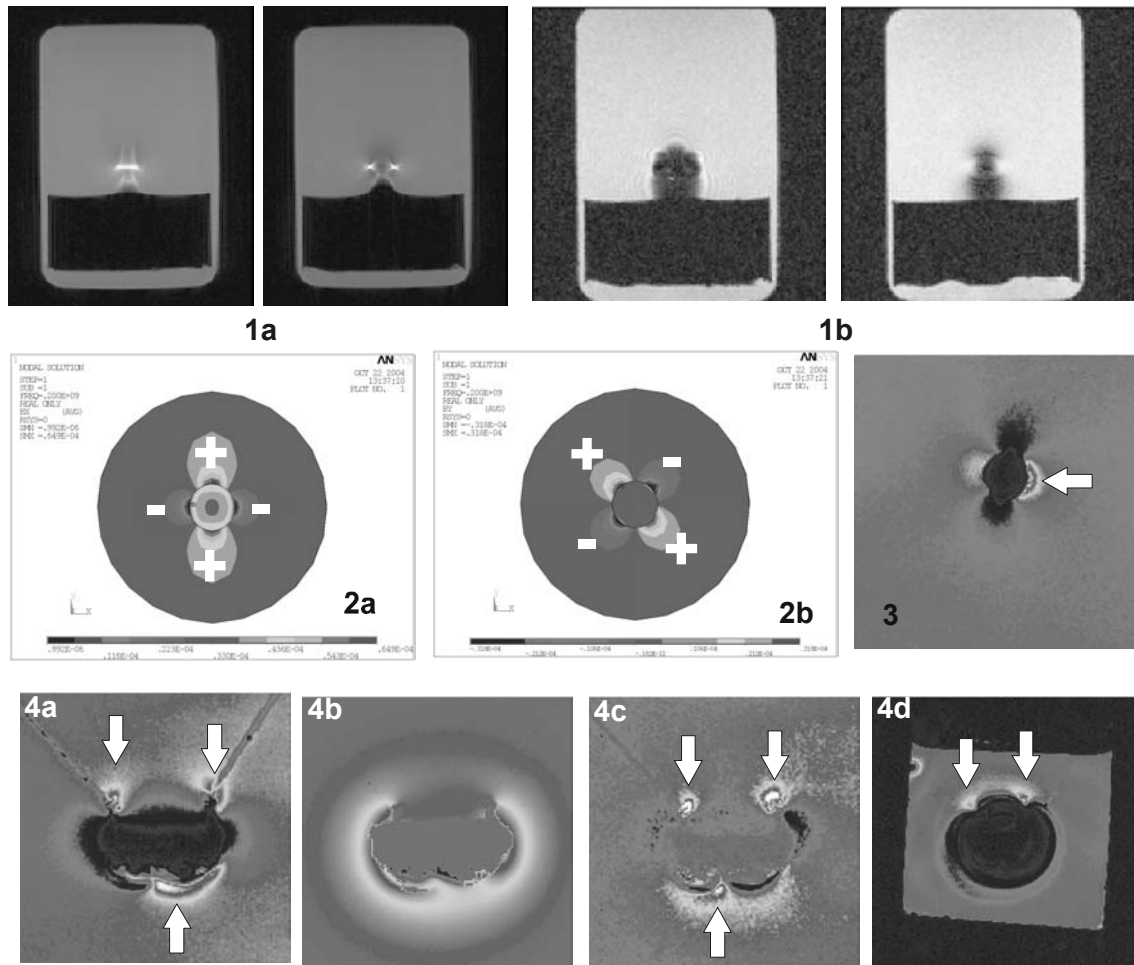
Fig. 1.  Images 1 show the typical artifacts found in (a) SE and (b) GE images, which can be explained by $B_0$ inhomogeneity around the sample (alloy rod protruding from the holder, 2 parallel slices shown, 1.5 T). In images 2, simulated $B_1$ field ($B_{1x}$, $B_{1y}$) generated by a linearly polarized $B_1$ coil around a conductive rod are displayed. $B_1$ values range between 0 (-) and 2× (+) the nominal value, which has been verified experimentally with an amalgam rod (magnitude image, image 3). The arrow points to $B_1$ peak area. In images 4, images (4.7T) of a suspended real precious-metal alloy crown show (a) a SE image, (b) $B_0$ shift (0-1.25ppm), (c) $B_1$ inhomogeneity, and (d) a GE image. The bright spots due to induced RF currents are marked by arrows. In the GE image only the 2 high-$B_1$ spots on the crown edge evaded a washout by intrapixel dephasing.

For quantitative assessment, 2D gradient-echo (TE=4.36ms) MRI in 4.7 T has been utilized, selecting 1-mm-thick perpendicular to $B_0$, intersecting centre of the sample, parallel with $B_0$. With the slice selection gradient of 90.5 mT/m (3860 Hz/mm) the slice deviation was <1mm, which was confirmed to be negligible by numerical modeling and by imaging orthogonal slices. The readout distortion (gradient of 20.0 mT/m, or 850 Hz/mm) was taken care of in data evaluation. The above outlined method was used for the determination of magnetic susceptibilities.

The electric conductivity was determined by standard electrotechnical measurements of the same cylindrical samples.

## 3. Results

The qualitative experimental findigs are illustrated by Fig. 1.

It has been found that precious-metal alloys and amalgams are slightly diamagnetic ($\chi$= -20x$10^{-6}$ to -40x$10^{-6}$) and do not influence the $B_0$ homogeneity significantly except in their very close vicinity. The highest conductivities were found in the group of precious-metal alloys (4.0-6.2 S.m/mm$^2$), while the conductivity of amalgams was marginally lower (3.4-4.1 S.m/mm$^2$). These properties make these materials prone to cause $B_1$ artifacts. The Co-Cr and Ni-Cr alloys were found highly paramagnetic ($\chi$=370x$10^{-6}$ to 1370x$10^{-6}$) and less conductive (0.80-1.3 S.m/mm$^2$). As a result, these materials lead to large $B_0$ inhomogeneities, overshadowing any $B_1$ effects. Large differences exist, however, within this group.

## 4. Discussion and Conclusions

The experimental results are consistent with model-based predictions. In most cases $B_0$ effects are predominant, but with materials of low magnetic susceptibility, flip angle modification due to induced RF currents becomes conspicuous. With highly paramagnetic materials, loss of signal due to intrapixel/intraslice dephasing occurs around the metallic objects in GE images, complex artifacts (including bright spots, stripes and black holes) arise in SE images, for which slice selection and position encoding distortions are responsible. In GE images, the diagnostic information is likely to be destroyed, but hardly any risk of misinterpretation arises. Misinterpretation of the artifacts is possible, however, in SE images. $B_1$ artifacts occur very close to the metallic objects, they may indicate the hot spots on the object and be contribute to MR safety assessment of the implant.

## Acknowledgements

## References

[1] Balac S., Caloz G,: Mathematical modeling and numerical simulation of magnetic susceptibility artifacts in MRI. http://citeseer.ist.psu.edu/balac00mathematical.html

[2] Deville G., Bernier M., Delrieux J.: *Phys. Rev.* B 19, 5666 (1979)

[3] Marques J. P. , Bowtell R.: Evaluation of a Fourier based method for calculating susceptibility induced magnetic field perturbations. *Proc. Intl. Soc. Mag. Reson. Med.* 11 (2003), p.1020.